DOI: https://doi.org/10.17816/DD629352

Use of radiomics and dosiomics to identify predictors of radiation-induced lung injury

Nikolay V. Nudnov[1,2,3], Vladimir M. Sotnikov[1], Mikhail E. Ivannikov[1], Elina S-A. Shakhvalieva[1], Aleksandr A. Borisov[1], Vasiliy V. Ledenev[4], Aleksei Yu. Smyslov[1], Alina V. Ananina[1]

[1] Russian Scientific Center of Roentgenoradiology, Moscow, Russia;
[2] Russian Medical Academy of Continuous Professional Education, Moscow, Russia;
[3] Peoples' Friendship University of Russia, Moscow, Russia;
[4] Central Clinical Military Hospital, Moscow, Russia

ABSTRACT

BACKGROUND: Radiomics is a machine learning-based technology that extracts, analyzes, and interprets quantitative features from digital medical images. In recent years, dosiomics has become an increasingly common term in the literature to describe a new radiomics method. Dosiomics is a texture analysis method for evaluating radiotherapy dose distribution patterns. Most of the published research in dosiomics evaluates its use in predicting radiation-induced lung injury.

AIM: The aim of the study was to identify predictors (biomarkers) of radiation-induced lung injury using texture analysis of computed tomography (CT) images of lungs and chest soft tissues using radiomics and dosiomics.

MATERIALS AND METHODS: The study used data from 36 women with breast cancer who received postoperative conformal radiation therapy. Retrospectively, the patients were divided into two groups according to the severity of post-radiation lung lesions. 3D Slicer was used to evaluate CT results of all patients obtained during radiation treatment planning and radiation dose distribution patterns. The software was able to unload radiomic and dosiomic features from regions of interest. The regions of interest included chest soft tissue and lung areas on the irradiated side where the dose burden exceeded 3 and 10 Gy.

RESULTS: The first group included 13 patients with minimal radiation-induced lung lesions, and the second group included 23 patients with post-radiation pneumofibrosis. In the lung area on the side irradiated with more than 3 Gy, statistically significant differences between the patient groups were obtained for three radiomic features and one dosiomic feature. In the lung area on the side irradiated with more than 10 Gy, statistically significant differences were obtained for 12 radiomic features and 1 dosiomic feature. In the area of chest soft tissues on the irradiated side, significant differences were obtained for 18 radiomic features and 4 dosiomic features.

CONCLUSION: As a result, a number of radiomic and dosiomic features were identified which were statistically different in patients with minimal lesions and pulmonary pneumofibrosis following radiation therapy for breast cancer. Based on texture analysis, predictors (biomarkers) were identified to predict post-radiation lung injury and identify higher-risk patients.

Keywords: dosiomics; radiomics; radiation therapy; texture analysis; post-radiation pneumonitis.

To cite this article:
Nudnov NV, Sotnikov MV, Ivannikov ME, Shakhvalieva ES-A, Borisov AA, Ledenev VV, Smyslov AYu, Ananina AV. Use of radiomics and dosiomics to identify predictors of radiation-induced lung injury. *Digital Diagnostics.* 2024;5(4):752–764. DOI: https://doi.org/10.17816/DD629352

Received: 23.03.2024 **Accepted:** 15.05.2024 **Published online:** 20.11.2024

DOI: https://doi.org/10.17816/DD629352

Опыт применения методов радиомики и дозиомики для нахождения предикторов лучевых повреждений лёгких

Н.В. Нуднов[1,2,3], В.М. Сотников[1], М.Е. Иванников[1], Э.С-А. Шахвалиева[1], А.А. Борисов[1], В.В. Леденёв[4], А.Ю. Смыслов[1], А.В. Ананьина[1]

[1] Российский научный центр рентгенорадиологии, Москва, Россия;
[2] Российская медицинская академия непрерывного профессионального образования, Москва, Россия;
[3] Российский университет дружбы народов имени Патриса Лумумбы, Москва, Россия;
[4] Центральный клинический военный госпиталь, Москва, Россия

АННОТАЦИЯ

Обоснование. Радиомика — это технология извлечения, анализа и интерпретации количественных характеристик из цифровых медицинских изображений, основанная на машинном обучении. В последние годы в литературе всё чаще встречается термин «дозиомика», обозначающий новое направление в радиомике. Дозиомика — это метод текстурного анализа планов распределения дозы облучения при лучевой терапии. Бóльшая часть опубликованных исследований в области дозиомики посвящена её применению в прогнозировании лучевого повреждения лёгких.

Цель — выявление предикторов (биомаркёров) лучевых повреждений лёгких с помощью текстурного анализа (методами радиомики и дозиомики) изображений лёгких, а также мягких тканей грудной клетки, полученных с помощью компьютерной томографии.

Материалы и методы. В исследовании использовали данные 36 женщин с раком молочной железы, прошедших послеоперационный курс конформной лучевой терапии. Ретроспективно пациенток разделили на две группы по степени постлучевых изменений лёгких. Результаты компьютерной томографии всех пациенток, полученные на этапе планирования лучевой терапии, и планы распределения доз облучения анализировали с помощью программного обеспечения 3D Slicer с функцией выгрузки показателей радиомики и дозиомики из областей интереса. В качестве областей интереса выбирали область мягких тканей грудной клетки и области лёгкого на стороне облучения, дозовая нагрузка на которые превышала 3 и 10 Гр.

Результаты. В первую группу включили 13 пациенток с минимальными постлучевыми изменениями в лёгких, во вторую группу — 23 пациентки с постлучевым пневмофиброзом. В области лёгкого на стороне облучения с дозовой нагрузкой более 3 Гр статистически значимые различия между группами пациенток получены по трём показателям радиомики и одному показателю дозиомики. В области лёгкого на стороне облучения с дозовой нагрузкой более 10 Гр статистически значимые различия получены по 12 показателям радиомики и 1 показателю дозиомики. В области мягких тканей грудной клетки на стороне облучения значимые различия получены по 18 показателям радиомики и 4 показателям дозиомики.

Заключение. В результате выполненного исследования получен ряд показателей радиомики и дозиомики, статистически различающихся у пациенток с минимальными постлучевыми изменениями и постлучевым пневмофиброзом лёгких после проведения лучевой терапии по поводу рака молочной железы. Предикторы (биомаркёры), выявленные нами на основе текстурного анализа, можно использовать для прогнозирования постлучевых повреждений лёгких и выявления пациентов с более высоким риском их развития.

Ключевые слова: дозиомика; радиомика; лучевая терапия; текстурный анализ; постлучевой пневмонит.

Как цитировать:
Нуднов Н.В., Сотников В.М., Иванников М.Е., Шахвалиева Э.С-А., Борисов А.А., Леденёв В.В., Смыслов А.Ю., Ананьина А.В. Опыт применения методов радиомики и дозиомики для нахождения предикторов лучевых повреждений лёгких // Digital Diagnostics. 2024. Т. 5, № 4. С. 752–764. DOI: https://doi.org/10.17816/DD629352

Рукопись получена: 23.03.2024 **Рукопись одобрена:** 15.05.2024 **Опубликована online:** 20.11.2024

DOI: https://doi.org/10.17816/DD629352

放射组学和剂量组学在寻找肺辐射损伤预测因数方面的应用经验

Nikolay V. Nudnov[1,2,3], Vladimir M. Sotnikov[1], Mikhail E. Ivannikov[1], Elina S-A. Shakhvalieva[1], Aleksandr A. Borisov[1], Vasiliy V. Ledenev[4], Aleksei Yu. Smyslov[1], Alina V. Ananina[1]

[1] Russian Scientific Center of Roentgenoradiology, Moscow, Russia;
[2] Russian Medical Academy of Continuous Professional Education, Moscow, Russia;
[3] Peoples' Friendship University of Russia, Moscow, Russia;
[4] Central Clinical Military Hospital, Moscow, Russia

摘要

论证。放射组学是一种基于机器学习从数字医学影像中提取、分析和解释定量特征的技术。近年来，“剂量组学”一词在文献中越来越常见，标志着放射组学的新方向。剂量组学是一种对放射治疗过程中辐射剂量分布计划进行纹理分析的方法。剂量组学领域已发表的大多数研究都致力于其在预测辐射引起的肺损伤中的应用。

目的 — 利用放射组学的纹理方法和肺部图像的剂量组学分析，以及计算机断层扫描获得的胸部软组织，从而确定肺部辐射损伤的预测因数（生物标志物）。

材料和方法。研究中，使用了36名接受术后适形放射治疗的乳腺癌妇女的数据。根据放疗后肺部变化的程度回顾性地将患者分为两组。使用3D Slicer软件对所有患者在放疗计划阶段获得的CT扫描结果和辐射剂量分布计划进行分析，该软件具有上传研究区域的放射组学和剂量组学指标的功能。选择照射一侧的胸部软组织和肺部区域作为研究区域，剂量负荷分别超过3 Gy和10 Gy。

结果。第一组包括13名放疗后肺部变化最小的患者，第二组包括23名放疗后肺纤维化的患者。在剂量负荷超过3 Gy的照射侧肺区，三项放射组学指标和一项剂量组学指标在患者组间存在显著统计学差异。在剂量负荷超过10 Gy的照射侧肺区，12项放射组学指标和1项剂量组学指标存在显著统计学差异。在照射一侧的胸部软组织区域，18项放射组学指标和4项剂量组学指标存在显著差异。

结论。研究结果表明，在乳腺癌放疗后、肺部放疗后微小变化和放疗后肺纤维化的患者中，一系列的放射组学和剂量组学指标存在统计学差异。我们根据纹理分析确定的预测因数（生物标志物）可用于预测放射后肺损伤，并确定发生肺损伤的发展风险较高的患者。

关键词：剂量组学；放射组学；放疗；纹理分析；放疗后肺炎。

引用本文：
Nudnov NV, Sotnikov MV, Ivannikov ME, Shakhvalieva ES-A, Borisov AA, Ledenev VV, Smyslov AYu, Ananina AV. 放射组学和剂量组学在寻找肺辐射损伤预测因数方面的应用经验. *Digital Diagnostics.* 2024;5(4):752–764. DOI: https://doi.org/10.17816/DD629352

收到：23.03.2024 **接受：**15.05.2024 **发布日期：**20.11.2024

BACKGROUND

Radiation therapy is a widely used method in cancer treatment [1]. However, it carries the risk of radiation-induced lung injury, particularly in patients with thoracic tumors. To mitigate this complication, various studies have explored the development of prognostic models using clinical, radiomic, and other relevant parameters [2].

Radiomics is an emerging technique based on texture analysis that evaluates quantitative image features to support the interpretation of medical images. It extracts image biomarkers that reflect abnormal changes from DICOM-format medical images. In this study, radiomic features were extracted using the open-source PyRadiomics library (AIM, USA). Radiomic features are generally categorized into two groups: first-order statistics and texture matrices related to co-occurrence and uniformity. These texture matrices include the following:

- Gray Level Co-occurrence Matrix (GLCM)
- Gray Level Run Length Matrix (GLRLM)
- Gray Level Size Zone Matrix (GLSZM)
- Neighboring Gray Tone Difference Matrix (NGTDM)
- Gray Level Dependence Matrix (GLDM) [3, 4].

A comprehensive explanation of these parameters and the formulas used for their calculation is available at pyradiomics.readthedocs.io [4].

Current evidence supports the utility of radiomics in predicting disease progression and treatment-related complications [5].

The term *dosiomics*, introduced by Gabryś et al. [6], is now widely used to describe a subfield within radiomics. Dosiomics applies texture analysis techniques to assess patterns in radiotherapy dose distributions. Similar to radiomic features, dosiomic features include co-occurrence and uniformity matrices that represent spatial relationships among pixels and voxels within an image. Most international studies on dosiomics have concentrated on its application in predicting radiation-induced lung injury [7].

The reported incidence of radiation-induced lung injury varies between 5% and 58% [8]. Risk factors for this condition can be categorized into two main groups. The first group comprises treatment-related factors, such as total radiation dose, dose fractionation, the volume of lung tissue exposed, the irradiation technique used, and the administration of chemotherapy or immunotherapy. The second group includes patient-related factors, such as age, smoking status, preexisting interstitial lung disease or chronic obstructive pulmonary disease, the location of the irradiated tumor, and individual, genetically determined radiosensitivity [9].

Radiation-induced lung injury progresses in two stages [10]. The first stage, known as postradiation pneumonitis or pulmonitis, is characterized by acute interstitial inflammation of lung tissue and typically occurs within 3–6 weeks after radiation therapy [11]. The second stage develops over the following 6 months, during which the acute changes may completely resolve or, especially at doses ⩾30 Gy, evolve into chronic changes of varying severity. In such cases, edema and infiltration may lead to irreversible postradiation pneumofibrosis [12, 13]. The diagnosis of postradiation pneumonitis is based on three key criteria: a prior history of radiation therapy; the presence of symptoms such as fever, cough with mucoid sputum, and dyspnea; and characteristic findings on computed tomography (CT) scans [14]. Typical CT features include initial ground-glass opacities, followed by areas of consolidation, fibrous bands, and in some cases, aerial bronchograms and traction bronchiectasis [12, 15]. Postradiation pneumonitis negatively impacts both quality of life and survival in cancer patients [9]. Enhancing radiation therapy techniques to achieve effective local tumor control while minimizing radiation exposure to surrounding lung tissue can reduce the risk of radiation-induced lung injury [16].

AIM

To identify predictors of radiation-induced lung injury by performing texture analysis of CT images of the lungs and chest soft tissues obtained prior to radiation therapy, using radiomic and dosiomic methods.

MATERIALS AND METHODS

Study design

This was a single-center, retrospective study involving the analysis of chest CT scans from patients with breast cancer.

Eligibility criteria

The study included patients with breast cancer who underwent postoperative conformal radiotherapy at the Russian Scientific Center of Roentgenology and Radiology between 2022 and 2023. The inclusion criterion was the availability of follow-up chest CT data obtained at least 6 months after radiation therapy, recorded in the Radiology Information System of the same center. These CT scans were used to assess the extent of postradiation lung changes. Participants were grouped based on the severity of these changes, as determined by the conclusions of an independent radiologist.

Intervention

Pre-radiation preparation included a chest CT scan performed on a SOMATOM Definition AS scanner (Siemens, Germany), followed by volumetric dosimetric planning for radiation therapy. Irradiation of the chest wall and tumor bed was carried out using the TrueBeam system (Varian MS, USA) with a total equivalent radiation dose ranging from 50 to 60 Gy. A follow-up chest CT scan was conducted no earlier than 6 months after the completion of radiation therapy.

Main study outcome

The study's null hypothesis assumed no statistically significant differences between groups in any of the 107 evaluated radiomic and dosiomic features.

Outcomes registration

CT images acquired during radiation therapy planning, along with corresponding dose distribution data, were processed using 3D Slicer software (3D Slicer Community). This software enabled the extraction of radiomic and dosiomic features from defined regions of interest [17]. Features were calculated for chest soft tissues within the irradiation zone along the anterior surface, as well as for lung regions that received radiation doses exceeding 3 Gy and 10 Gy. Regions of interest were identified semi-automatically using Varian software (Varian, USA). For each region, 107 radiomic and dosiomic features were extracted, including first-order statistics, shape descriptors, and texture matrices related to co-occurrence and uniformity.

Subgroup analysis

Participants were retrospectively divided into two groups based on follow-up chest CT findings obtained 6 months after radiation therapy. Group 1 consisted of patients with minimal postradiation changes, while Group 2 included those with pronounced postradiation pneumofibrosis.

Ethics approval

The study protocol was reviewed and approved by the Independent Ethics Committee of the Russian Scientific Center of Roentgenology and Radiology on March 1, 2024 (Meeting Minutes No. 2).

Statistical analysis

The sample size was not predetermined. Data processing and statistical analysis were performed using Microsoft Office Excel and R-Studio, an open-source development environment for the R programming language (Posit, USA). The Mann–Whitney U test and Fisher's exact test were used to evaluate differences in quantitative and qualitative variables, respectively. Data are reported as the median along with the 25th and 75th percentiles (first and third quartiles). A p-value of <0.05 was considered statistically significant.

RESULTS

Participants

The study analyzed pre-radiation therapy CT scans of the lungs and chest soft tissues from 36 patients with breast cancer.

Group 1 consisted of 13 patients who exhibited minimal postradiation changes (Fig. 1*a*), while Group 2 included 23 patients with severe postradiation pneumofibrosis (Fig. 1*b*).

Quantitative and qualitative parameter comparisons between the two groups are shown in Tables 1 and 2.

The results support the validity of the intergroup comparisons.

Primary results

For the calculation of radiomic and dosiomic features, regions of interest on CT scans were selected based on a radiomic dose threshold of 3 Gy. This threshold was chosen based on previous studies showing that doses between 0 and 3 Gy do not lead to radiation-induced lung injury [13]. Additionally, some international studies consider a 3 Gy dose as a potential predictor of pneumonitis [18]. In texture analysis involving large tissue volumes, radiomic features are averaged, which can obscure significant differences and occasionally lead to missing relevant texture parameters in small regions of interest. Therefore, an additional threshold dose of 10 Gy was used to improve accuracy.

In the lung regions exposed to radiation doses greater than 3 Gy, significant differences were observed in three radiomic features and one dosiomic feature. The comparisons of these parameters—including median values, first and third quartiles, and statistical significance levels—are presented in Table 3.

The GLSZM Size Zone Nonuniformity values suggest that patients in Group 2 (with postradiation pneumofibrosis) exhibited more uniform gray level zone volumes. This is in line with findings for NGTDM Busyness, which measures

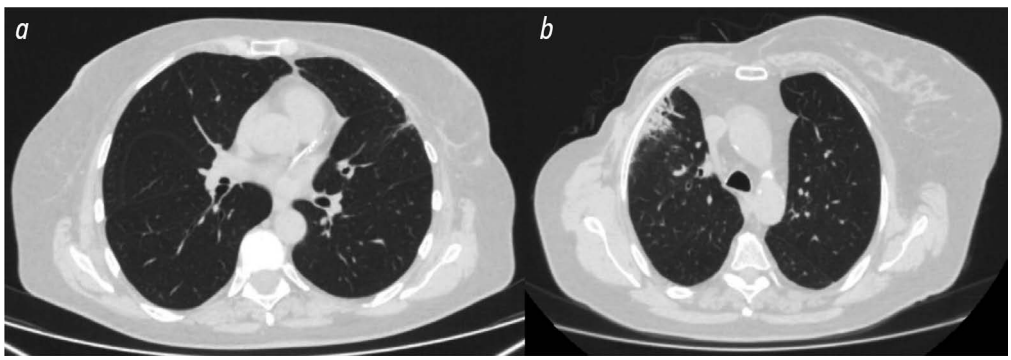

Fig. 1. Chest computed tomography at 6 months postradiation therapy: *a*, minimal postradiation changes in the left lung; *b*, severe postradiation pneumofibrosis in the right lung.

Table 1. Comparison of study groups by quantitative parameters

Parameter		Group 1 (minimal postradiation changes)	Group 2 (postradiation pneumofibrosis)	*p*-value
Age, years		61 [54; 67]	65 [55; 72]	0.179
Irradiated lung volume, cm^3, radiation exposure	>3 Gy	945.94 [781.81; 1175.68]	828.67 [668.27; 1032.38]	0.190
	>10 Gy	613.88 [420.02; 694.52]	527.27 [403.10; 611.62]	0.344
	>30 Gy	330.36 [239.15; 449.71]	354.03 [248.07;447.64]	0.771

Note. Data are presented as Me [Q1; Q3], where Me is the median, Q1 is the first quartile, and Q3 is the third quartile.

Table 2. Comparison of study groups by qualitative parameters

Parameter		Number of patients (% of the total number of patients in the group)		*p*-value
		Group 1 (minimal postradiation changes)	Group 2 (postradiation pneumofibrosis)	
Smoking status		0	0	–
Concomitant lung diseases		1 (7,7)	0	0.361
Concomitant heart disease		5 (38,5)	10 (43.5)	0.526
History of chemotherapy		8 (61,5)	15 (65.2)	0.821
Affected mammary gland	Left	6 (46.1)	12 (52.2)	0.5
	Right	7 (53.8)	11 (47.8)	
Disease stage	T1–4N1–3M0	10 (76.9)	12 (52.2)	0.175
	T1–3N0M0	3 (23.1)	11 (47.8)	
Surgery type	Radical mastectomy	7 (53.8)	15 (65.2)	0.480
	Partial mastectomy	6 (46.1)	7 (30.4)	

Note. Disease stage is indicated according to the TNM staging system, where T0–4 (tumor) represents the size of the primary tumor, N0–3 (nodes) refers to the degree of spread to regional lymph nodes, and M0–1 (metastasis) indicates the presence of distant metastasis.

Table 3. Comparison of the two patient groups by radiomic and dosiomic features in lung fields with radiation exposure exceeding 3 Gy

Parameter	Group 1 (minimal postradiation changes)	Group 2 (postradiation pneumofibrosis)	*p*-value
Radiomic features			
GLRLM Gray Level Nonuniformity	17 464.52 [12199.53; 26481.37]	11 904.86 [7059.69; 20646.00]	0.05
GLSZM Size Zone Nonuniformity	19 096.83 [15693.52; 23905.24]	13 307.97 [11842.68; 19368.63]	0.043
NGTDM Busyness	74.81 [55.15; 102.73]	56.56 [34.50; 78.11]	0.047
Dosiomic features			
GLCM Maximum Probability	0.60 [0.55; 0.68]	0.55 [0.53; 0.61]	0.05

Note. Data are presented as Me [Q1; Q3], where Me is the median, Q1 is the first quartile, and Q3 is the third quartile. GLRLM, Gray Level Run Length Matrix; GLSZM, Gray Level Size Zone Matrix; NGTDM, Neighboring Gray Tone Difference Matrix; GLCM, Gray Level Co-occurrence Matrix.

the heterogeneity of adjacent pixels and was higher in Group 1 (patients with minimal postradiation changes). These results may indicate that lung tissue in Group 1, which demonstrates better recovery from radiation injury, has more distinct gray level variations and is less likely to form large homogeneous areas. Early postradiation pneumonitis on CT is typically characterized by local interstitial inflammation and damage to the microvascular endothelium [19, 20]. The baseline condition of the pulmonary microvasculature may influence the tissue's ability to recover from radiation injury, and the observed texture features may reflect the degree of vascular development.

In the lung regions receiving more than 10 Gy of radiation, significant differences were identified in 12 radiomic features and 1 dosiomic feature. The comparisons for these parameters are summarized in Table 4.

For instance, the GLCM Cluster Shade, which reflects the heterogeneity of gray level cluster distribution, was approximately 44% higher in patients with postradiation pneumofibrosis. This is further supported by the GLCM Cluster Prominence values, which indicate that in Group 1 (patients with minimal radiation-induced injury), the gray levels within clusters are closer to the overall average for lung tissue. In contrast, Group 2 (patients with postradiation

Table 4. Comparison of the two patient groups by radiomic and dosiomic features in lung fields with radiation exposure exceeding 10 Gy

Parameter	Group 1 (minimal postradiation changes)	Group 2 (postradiation pneumofibrosis)	*p*-value
Radiomic features			
Flatness	0.23 [0.22; 0.25]	0.26 [0.24; 0.29]	0.040
First-order Mean Absolute Deviation	112.38 [97.82; 152.24]	129.81 [118.67; 153.71]	0.048
GLCM Cluster Prominence	186 230.89 [148727.18; 306231.09]	321 625.90 [230877.79; 417140.54]	0.028
GLCM Cluster Shade	3366.36 [2860.31; 5779.96]	5998.08 [4269.97; 6497.98]	0.037
GLCM Cluster Tendency	105.53 [84.37; 171.43]	156.66 [122.25; 179.47]	0.048
GLCM Correlation	0.55 [0.49; 0.60]	0.59 [0.55; 0.63]	0.048
GLCM Sum Squares	34.48 [27.65; 54.08]	46.15 [37.78; 55.89]	0.044
GLDM Dependence Entropy	7.10 [6.95; 7.21]	7.19 [7.03; 7.34]	0.056
GLRLM High Gray Level Run Emphasis	149.91 [129.33; 200.75]	176.32 [159.08; 199.05]	0.044
GLRLM Run Entropy	4.85 [4..70; 5.00]	5.01 [4.85; 5.08]	0.024
GLRLM Short Run High Gray Level Emphasis	143.26 [121.04; 193.03]	168.49 [152.61; 191.58]	0.048
GLSZM Zone Entropy	6.63 [6.55; 6.73]	6.75 [6.67; 6.81]	0.031
Dosiomic features			
NGTDM Flatness	0.23 [0.22; 0.25]	0.26 [0.24; 0.30]	0.040

Note. Data are presented as Me [Q1; Q3], where Me is the median, Q1 is the first quartile, and Q3 is the third quartile. GLCM, Gray Level Co-occurrence Matrix; GLDM, Gray Level Dependence Matrix; GLRLM, Gray Level Run Length Matrix; GLSZM, Gray Level Size Zone Matrix; NGTDM, Neighboring Gray Tone Difference Matrix.

pneumofibrosis) showed over 40% greater variability in gray level distribution within individual clusters. These results suggest that, at baseline, patients in Group 2 had more areas of increased density and heterogeneity compared to the more uniform lung tissue in Group 1. The GLRLM High Gray Level Run Emphasis shows that Group 2 had 15% more regions with high gray levels, suggesting denser lung tissue at baseline in patients who later developed significant postradiation changes. This observation aligns with previous studies [13]. Morphologically, this could be associated with a greater presence of fibrotic lung areas before treatment.

In the irradiated chest soft tissues, significant differences between groups were found in 18 radiomic features (Table 5) and 4 dosiomic features (Table 6).

As shown in Table 5, significant intergroup differences were observed in the texture parameters. For instance, GLSM autocorrelation, which measures texture fineness or coarseness, was 42% higher in Group 2. GLSZM Large Area Emphasis, which indicates coarser texture in large areas, was 46% higher in Group 1. NGTDM Busyness, which reflects intensity changes between neighboring pixels, was 31% higher in Group 1. The latter two parameters suggest that Group 1 has a less uniform texture with sharper intensity changes.

Table 6 shows that Group 2 had higher total GLCM Entropy, indicating more significant intensity variations in the image. The GLRLM Long Run Low Gray Level Emphasis, which reflects the distribution of low gray level values, was higher in Group 1, suggesting a greater number of low gray level values in the image. The larger number of parameters with intergroup differences (Tables 5 and 6) suggests that the condition of chest soft tissues and mammary glands could serve as predictors of lung tissue recovery following radiation therapy. However, the underlying mechanisms and nature of this association require further study.

DISCUSSION

The variety of risk factors for radiation-induced lung injury allows for the use of different quantitative and qualitative parameters to predict this complication. For instance, Zhao et al. [21] found that elevated levels of transforming growth factor beta (TGF-β) in the blood within the first 4 weeks of radiation therapy could predict the risk of lung injury with 66.7% sensitivity and 95.0% specificity. Chen et al. [22] developed a model based on an artificial neutral network to predict the risk of postradiation pneumonitis using factors such as the volume of lung tissue exposed to >16 Gy, cumulative equivalent uniform dose, forced expiratory volume in 1 s, diffusing capacity for carbon monoxide, and chemotherapy history. Additionally, many researchers have applied radiobiological models to predict the risk of radiation-induced damage to healthy tissues [23].

Table 5. Comparison of the two patient groups by radiomic features in irradiated chest soft tissues

Parameter	Group 1 (minimal postradiation changes)	Group 2 (postradiation pneumofibrosis)	*p*-value
GLCM Autocorrelation	327.37 [26.23; 716.81]	778.92 [250.21; 1299.00]	0.04
GLCM Joint Average	17.92 [5.00; 26.57]	27.83 [15.66; 36.00]	0.04
GLCM SumAverage	35.85 [10.00; 53.15]	55.67 [31.32; 72.01]	0.04
GLDM High Gray Level Emphasis	330.75 [26.84; 722.33]	785.17 [252.23; 1301.19]	0.04
GLDM Large Dependence High Gray Level Emphasis	34,520.55 [4229.63; 90 474.35]	94,735.42 [34,425.42; 178,891.14]	0.031
GLDM Small Dependence Emphasis	0.04 [0.04; 0.05]	0.06 [0.04; 0.06]	0.031
GLDM Small Dependence High Gray Level Emphasis	15.94 [1.32; 36.06]	40.80 [14.16; 69.29]	0.034
GLRLM High Gray Level Run Emphasis	337.14 [29.46; 731.67]	786.90 [257.09; 1312.39]	0.044
GLRLM Long Run High Gray Level Emphasis	1047.96 [132.06; 2600.37]	2816.82 [992.76; 5222.59]	0.028
GLRLM Short Run High Gray Level Emphasis	259.01 [20.99; 561.86]	573.11 [186.60; 970.35]	0.048
GLSZM Gray Level NonUniformity Normalized	0.13 [0.09; 0.20]	0.10 [0.07; 0.11]	0.031
GLSZM Large Area Emphasis	1,738,981.12 [415,642.22; 3,268,243.47]	815,272.55 [212,074.04; 1,207,397.63]	0.048
GLSZM Large Area Low Gray Level Emphasis	8843.95 [1392.9; 148,364.17]	1025.44 [474.68; 4267.21]	0.011
GLSZM Small Area High Gray Level Emphasis	232.12 [27.48; 493.15]	517.89 [205.88; 828.21]	0.044
GLSZM Zone Percentage	0.03 [0.03; 0.04]	0.04 [0.03; 0.05]	0.044
GLSZM Zone Variance	1,737,696.14 [414,536.61; 3,266,421.34]	814,359.34 [211,603.3; 1,206,631.61]	0.048
NGTDM Busyness	25.52 [9.61; 135.47]	8.10 [4.51; 17.92]	0.012
NGTDM Strength	0.09 [0.05; 0.25]	0.28 [0.15; 0.54]	0.037

Note. Data are presented as Me [Q1; Q3], where Me is the median, Q1 is the first quartile, and Q3 is the third quartile. GLCM, Gray Level Co-occurrence Matrix; GLDM, Gray Level Dependence Matrix; GLRLM, Gray Level Run Length Matrix; GLSZM, Gray Level Size Zone Matrix; NGTDM, Neighboring Gray Tone Difference Matrix.

Table 6. Comparison of the two patient groups by dosiomic features in irradiated chest soft tissues

Parameter	Group 1 (minimal postradiation changes)	Group 2 (postradiation pneumofibrosis)	*p*-value
GLCM SumEntropy	1.10 [0.55; 1.23]	1.26 [0.65; 1.31]	0.05
GLRLM Long Run Low Gray Level Emphasis	64.07 [39.55; 120.07]	38.78 [25.75; 55.68]	0.028
GLRLM Short Run High Gray Level Emphasis	0.40 [0.25; 0.49]	0.47 [0.42; 0.94]	0.026
NGTDM Complexity	0.06 [0.04; 0.07]	0.08 [0.06; 0.25]	0.05

Note. Data are presented as Me [Q1; Q3], where Me is the median, Q1 is the first quartile, and Q3 is the third quartile. GLCM, Gray Level Co-occurrence Matrix; GLRLM, Gray Level Run Length Matrix; NGTDM, Neighboring Gray Tone Difference Matrix.

Radiomics may enhance the prognostic value of predictive models. For example, Wang et al. [24] developed a radiomics nomogram with a concordance index of 0.921. Several studies on predicting the risk of radiation-induced lung injury have shown that models incorporating radiomic and dosiomic features are highly effective [7]. A key study by Huang et al. [18] reported a prognostic model that combined dosiomic and radiomic features with a high prognostic value (AUC 0.9). Importantly, including clinical findings in prognostic models further improves their performance [25]. Comparative studies examining

the effectiveness of dosimetry parameters (which describe the radiation therapy received) versus dosiomic features suggest that dosiomics can be integrated into prognostic models [26–28]. Adachi et al. [29] found that combining dosimetry parameters with dosiomic features enhanced the prognostic value of models. Based on international research, combined models using dosiomics, radiomics, clinical findings, and dosimetry can be a powerful prognostic tool [25, 30].

The studies mentioned above support our results, showing significant differences in radiomic and dosiomic features between patients with minimal postradiation changes and those with postradiation pneumofibrosis. These differences, identified before radiation therapy, were predictive of the risk of postradiation pneumofibrosis.

Study limitations

This study has several notable limitations. First, the sample size is small, and we plan to address this in future research. Second, the study utilized images from a single CT scanner. This limitation could be overcome by conducting a multicenter study or using external datasets, though this would require additional standardization of image generation and processing. The third limitation is the lack of universally accepted criteria for differentiating between minimal postradiation changes and postradiation pneumofibrosis. This could be addressed by employing computer vision techniques to measure the volume of affected and unaffected lung tissue. While this is an experimental, pilot study, it provides promising results for future development.

CONCLUSION

The study identified several radiomic and dosiomic features that significantly differed between patients with minimal postradiation changes and those with postradiation pneumofibrosis after radiation therapy for breast cancer. These differences were observed in both lung tissue and irradiated chest soft tissues. The findings suggest that the risk of radiation-induced lung injury may be influenced by individual patient characteristics, including lung tissue structure and the status of chest soft tissues. The texture parameters identified in this study can help predict the risk of radiation-induced lung injury and identify high-risk patients. International research indicates that predicting the risk of radiation-induced lung injury should involve not only the texture parameters of CT images but also dosimetry, laboratory, and other clinical parameters. This approach will enable the most comprehensive, patient-specific assessment and lead to highly accurate prognostic models.

ADDITIONAL INFORMATION

Funding source. This study was not supported by any external sources of funding.

Competing interests. The authors declare that they have no competing interests.

Authors' contribution. All authors made a substantial contribution to the conception of the work, acquisition, analysis, interpretation of data for the work, drafting and revising the work, final approval of the version to be published and agree to be accountable for all aspects of the work. N.V. Nudnov, V.M. Sotnikov — design of the study and final proofreading of the manuscript; M.E. Ivannikov, E.S-A. Shakhvalieva, A.A. Borisov, V.V. Ledenev, A.Yu. Smyslov, A.V. Ananina — data collection and analysis, writing and editing of the manuscript.

Consent for publication. Written consent was obtained from the patient for publication of relevant medical information and all of accompanying images within the manuscript.

REFERENCES

1. Khmelevsky EV, Kaprin AD. The state of a radiotherapy service in Russia: Comparative analysis and prospects for development. *P.A. Herzen Journal of Oncology.* 2017;6(4):38-41. EDN: ZFCHGJ doi: 10.17116/onkolog20176438-41

2. Kuipers ME, van Doorn-Wink KCJ, Hiemstra PS, Slats AM. Predicting radiation-induced lung injury in lung cancer patients — challenges and opportunities: Predicting radiation-induced lung injury. *Int J Radiat Oncol Biol Phys.* 2023;118(3):639–649. doi: 10.1016/j.ijrobp.2023.10.044

3. Mayerhoefer ME, Materka A, Langs G, et al. Introduction to Radiomics. *J Nucl Med.* 2020;61(4):488–495. doi: 10.2967/jnumed.118.222893

4. Radiomic Features: pyradiomics v3.0.1.post15+g2791e23 documentation [Internet]. [cited 25 Nov 2023]. Available from: https://pyradiomics.readthedocs.io/en/latest/features.html#.

5. Avanzo M, Stancanello J, Pirrone G, Sartor G. Radiomics and deep learning in lung cancer. *Strahlenther Onkol.* 2020;196(10):879–887. doi: 10.1007/s00066-020-01625-9

6. Gabryś HS, Buettner F, Sterzing F, et al. Design and selection of machine learning methods using radiomics and dosiomics for normal tissue complication probability modeling of xerostomia. *Front Oncol.* 2018;8:35. doi: 10.3389/fonc.2018.00035

7. Solodkiy VA, Nudnov NV, Ivannikov ME, et al. Dosiomics in the analysis of medical images and prospects for its use in clinical practice. *Digital Diagnostics.* 2023;4(3):340–355. EDN: EQRWGJ doi: 10.17816/DD420053

8. Arroyo-Hernández M, Maldonado F, Lozano-Ruiz F, et al. Radiation-induced lung injury: Current evidence. *BMC Pulm Med.* 2021;21(1):9. doi: 10.1186/s12890-020-01376-4

9. Rahi MS, Parekh J, Pednekar P, et al. Radiation-Induced Lung Injury — Current Perspectives and Management. *Clin Pract.* 2021;11(3):410–429. doi: 10.3390/clinpract11030056

10. Yan Y, Fu J, Kowalchuk RO, et al. Exploration of radiation-induced lung injury, from mechanism to treatment: a narrative review. *Transl Lung Cancer Res.* 2022;11(2):307–322. doi: 10.21037/tlcr-22-108

11. Gladilina IA, Shabanov MA, Kravets OA, et al. Radiation-Induced Lung Injury. *Journal of oncology: diagnostic radiology and radiotherapy.* 2020;3(2):9–18. EDN: SKOAAY doi: 10.37174/2587-7593-2020-3-2-9-18

12. Nudnov NV, Sotnikov VM, Ledenev VV, Baryshnikova DV. Features a Qualitative Assessment of Radiation-Induced Lung Damage by CT. *Medical Visualization.* 2016;(1):39–46. EDN: VWOIIB
13. Ledenev VV. *Methodology for quantitative assessment of radiation damage to lungs in cancer patients using CT* [dissertation]. Moscow, 2023. Available from: https://www.rncrr.ru/nauka/dissertatsionnyy-sovet/obyavleniya-o-zashchitakh/upload%202023/Леденев_Диссертация.pdf (In Russ.) EDN: YBWROM
14. Zhou C, Yu J. Chinese expert consensus on diagnosis and treatment of radiation pneumonitis. *Prec Radiat Oncol.* 2022;6(3):262–271. doi: 10.1002/pro6.1169
15. Konkol M, Śniatała P, Milecki P. Radiation-induced lung injury — what do we know in the era of modern radiotherapy? *Rep Pract Oncol Radiother.* 2022;27(3):552–565. doi: 10.5603/RPOR.a2022.0046
16. Shaymuratov RI. Radiation-induced lung injury. A review. *The Bulletin of Contemporary Clinical Medicine.* 2020;13(3):63–73. EDN: BIZZHU doi: 10.20969/VSKM.2020.13(3).63-73
17. 3D Slicer image computing platform [Internet]. [cited 25 Nov 2023]. Available from: https://www.slicer.org/
18. Wang L, Gao Z, Li C, et al. Computed Tomography-Based Delta-Radiomics Analysis for Discriminating Radiation Pneumonitis in Patients With Esophageal Cancer After Radiation Therapy. *Int J Radiat Oncol Biol Phys.* 2021;111(2):443–455. doi: 10.1016/j.ijrobp.2021.04.047
19. Begosh-Mayne D, Kumar SS, Toffel S, et al. The dose-response characteristics of four NTCP models: using a novel CT-based radiomic method to quantify radiation-induced lung density changes. *Sci Rep.* 2020;10(1):10559. doi: 10.1038/s41598-020-67499-0
20. Korpela E, Liu SK. Endothelial perturbations and therapeutic strategies in normal tissue radiation damage. *Radiat Oncol.* 2014;9:266. doi: 10.1186/s13014-014-0266-7
21. Zhao L, Sheldon K, Chen M, et al. The predictive role of plasma TGF-beta1 during radiation therapy for radiation-induced lung toxicity deserves further study in patients with non-small cell lung cancer. *Lung Cancer.* 2008;59(2):232–239. doi: 10.1016/j.lungcan.2007.08.010
22. Chen S, Zhou S, Zhang J, et al. A neural network model to predict lung radiation-induced pneumonitis. *Med Phys.* 2007;34(9):3420–3427. doi: 10.1118/1.2759601
23. Jain V, Berman AT. Radiation Pneumonitis: Old Problem, New Tricks. *Cancers (Basel).* 2018;10(7):222. doi: 10.3390/cancers10070222
24. Huang Y, Feng A, Lin Y, et al. Radiation pneumonitis prediction after stereotactic body radiation therapy based on 3D dose distribution: Dosiomics and/or deep learning-based radiomics features. *Radiat Oncol.* 2022;17(1):188. doi: 10.1186/s13014-022-02154-8
25. Zhang Z, Wang Z, Yan M, et al. Radiomics and dosiomics signature from whole lung predicts radiation pneumonitis: A model development study with prospective external validation and decision-curve analysis. *Int J Radiat Oncol Biol Phys.* 2023;115(3):746–758. doi: 10.1016/j.ijrobp.2022.08.047
26. Puttanawarut C, Sirirutbunkajorn N, Khachonkham S, et al. Biological dosiomic features for the prediction of radiation pneumonitis in esophageal cancer patients. *Radiat Oncol.* 2021;16(1):220. doi: 10.1186/s13014-021-01950-y
27. Liang B, Yan H, Tian Y, et al. Dosiomics: Extracting 3D spatial features from dose distribution to predict incidence of radiation pneumonitis. *Front Oncol.* 2019;(9):269.doi: 10.3389/fonc.2019.00269
28. Liang B, Tian Y, Chen X, et al. Prediction of radiation pneumonitis with dose distribution: A convolutional neural network (CNN) based model. *Front Oncol.* 2020;9:1500. doi: 10.3389/fonc.2019.01500
29. Adachi T, Nakamura M, Shintani T, et al. Multi-institutional dose-segmented dosiomic analysis for predicting radiation pneumonitis after lung stereotactic body radiation therapy. *Med Phys.* 2021;48(4):1781–1791. doi: 10.1002/mp.14769
30. Zheng X, Guo W, Wang Y, et al. Multi-omics to predict acute radiation esophagitis in patients with lung cancer treated with intensity-modulated radiation therapy. *Eur J Med Res.* 2023;28(1):126. doi: 10.1186/s40001-023-01041-6

СПИСОК ЛИТЕРАТУРЫ

1. Хмелевский Е.В., Каприн А.Д. Состояние радиотерапевтической службы России: сравнительный анализ и перспективы развития // Онкология. Журнал им. П.А. Герцена. 2017. Т. 6, № 4. С. 38–41. EDN: ZFCHGJ doi: 10.17116/onkolog20176438-41
2. Kuipers M.E., van Doorn-Wink K.C.J., Hiemstra P.S., Slats A.M. Predicting radiation-induced lung injury in lung cancer patients — challenges and opportunities: Predicting radiation-induced lung injury // Int J Radiat Oncol Biol Phys. 2023. Vol. 118, N 3. P. 639–649. doi: 10.1016/j.ijrobp.2023.10.044
3. Mayerhoefer M.E., Materka A., Langs G., et al. Introduction to Radiomics // J Nucl Med. 2020. Vol. 61, N 4. P. 488–495. doi: 10.2967/jnumed.118.222893
4. Radiomic Features: pyradiomics v3.0.1.post15+g2791e23 documentation [Internet]. [дата обращения: 25.11.2023]. Режим доступа: https://pyradiomics.readthedocs.io/en/latest/features.html#
5. Avanzo M., Stancanello J., Pirrone G., et al. Radiomics and deep learning in lung cancer // Strahlenther Onkol. 2020. Vol. 196, N 10. P. 879–887. doi: 10.1007/s00066-020-01625-9
6. Gabryś H.S., Buettner F., Sterzing F., et al. Design and selection of machine learning methods using radiomics and dosiomics for normal tissue complication probability modeling of xerostomia // Front Oncol. 2018. Vol. 8. ID 35. doi: 10.3389/fonc.2018.00035
7. Солодкий В.А., Нуднов Н.В., Иванников М.Е., и др. Дозиомика в анализе медицинских изображений и перспективы её использования в клинической практике // Digital Diagnostics. 2023. Т. 4, № 3. С. 340–355. EDN: EQRWGJ doi: 10.17816/DD420053
8. Arroyo-Hernández M., Maldonado F., Lozano-Ruiz F., et al. Radiation-induced lung injury: Current evidence // BMC Pulm Med. 2021. Vol. 21, N 1. ID 9. doi: 10.1186/s12890-020-01376-4
9. Rahi M.S., Parekh J., Pednekar P., et al. Radiation-Induced Lung Injury — Current Perspectives and Management // Clin Pract. 2021. Vol. 11, N 3. P. 410–429. doi: 10.3390/clinpract11030056
10. Yan Y., Fu J., Kowalchuk R.O., et al. Exploration of radiation-induced lung injury, from mechanism to treatment: a narrative review // Transl Lung Cancer Res. 2022. Vol. 11, N 2. P. 307–322. doi: 10.21037/tlcr-22-108
11. Гладилина И.А., Шабанов М.А., Кравец О.А., и др. Постлучевые повреждения лёгких // Онкологический журнал: лучевая диагностика, лучевая терапия. 2020. Т. 3, № 2. С. 9–18. EDN: SKOAAY doi: 10.37174/2587-7593-2020-3-2-9-18

12. Нуднов Н.В., Сотников В.М., Леденёв В.В., Барышникова Д.В. Возможности качественной оценки лучевых повреждений лёгких методом компьютерной томографии // Медицинская визуализация. 2016. № 1. С. 39–46. EDN: VWOIIB
13. Леденёв В.В. Методика количественной оценки лучевых повреждений лёгких у онкологических пациентов по данным рентгеновской компьютерной томографии: диссертация на соискание учёной степени канд. мед. наук. Москва, 2023. 133 с. Режим доступа: https://www.rncrr.ru/nauka/dissertatsionnyy-sovet/obyavleniya-o-zashchitakh/upload%202023/Леденев_Диссертация.pdf Дата обращения: 25.11.2023. EDN: YBWROM
14. Zhou C., Yu J. Chinese expert consensus on diagnosis and treatment of radiation pneumonitis // Prec Radiat Oncol. 2022. Vol. 6, N 3. P. 262–271. doi: 10.1002/pro6.1169
15. Konkol M., Śniatała P., Milecki P. Radiation-induced lung injury — what do we know in the era of modern radiotherapy? // Rep Pract Oncol Radiother. 2022. Vol. 27, N 3. P. 552–565. doi: 10.5603/RPOR.a2022.0046
16. Шаймуратов Р.И. Радиационно-индуцированные поражения лёгких. Современное состояние проблемы // Вестник современной клинической медицины. 2020. Т. 13, № 3. С. 63–73. EDN: BIZZHU doi: 10.20969/VSKM.2020.13(3).63-73
17. 3D Slicer image computing platform [Internet]. [дата обращения: 25.11.2023]. Режим доступа: https://www.slicer.org/
18. Wang L., Gao Z., Li C., et al. Computed Tomography-Based Delta-Radiomics Analysis for Discriminating Radiation Pneumonitis in Patients With Esophageal Cancer After Radiation Therapy // Int J Radiat Oncol Biol Phys. 2021. Vol. 111, N 2. P. 443–455. doi: 10.1016/j.ijrobp.2021.04.047
19. Begosh-Mayne D., Kumar S.S., Toffel S., et al. The dose-response characteristics of four NTCP models: using a novel CT-based radiomic method to quantify radiation-induced lung density changes // Sci Rep. 2020. Vol. 10, N 1. ID 10559. doi: 10.1038/s41598-020-67499-0
20. Korpela E., Liu S.K. Endothelial perturbations and therapeutic strategies in normal tissue radiation damage // Radiat Oncol. 2014. Vol. 9. ID 266. doi: 10.1186/s13014-014-0266-7
21. Zhao L., Sheldon K., Chen M., et al. The predictive role of plasma TGF-beta1 during radiation therapy for radiation-induced lung toxicity deserves further study in patients with non-small cell lung cancer // Lung Cancer. 2008. Vol. 59, N 2. P. 232–239. doi: 10.1016/j.lungcan.2007.08.010
22. Chen S., Zhou S., Zhang J., et al. A neural network model to predict lung radiation-induced pneumonitis // Med Phys. 2007. Vol. 34, N 9. P. 3420–3427. doi: 10.1118/1.2759601
23. Jain V., Berman A.T. Radiation Pneumonitis: Old Problem, New Tricks // Cancers (Basel). 2018. Vol. 10, N 7. ID 222. doi: 10.3390/cancers10070222
24. Huang Y., Feng A., Lin Y., et al. Radiation pneumonitis prediction after stereotactic body radiation therapy based on 3D dose distribution: Dosiomics and/or deep learning-based radiomics features // Radiat Oncol. 2022. Vol. 17, N 1. ID 188. doi: 10.1186/s13014-022-02154-8
25. Zhang Z., Wang Z., Yan M., et al. Radiomics and dosiomics signature from whole lung predicts radiation pneumonitis: A model development study with prospective external validation and decision-curve analysis // Int J Radiat Oncol Biol Phys. 2023. Vol. 115, N 3. P. 746–758. doi: 10.1016/j.ijrobp.2022.08.047
26. Puttanawarut C., Sirirutbunkajorn N., Khachonkham S., et al. Biological dosiomic features for the prediction of radiation pneumonitis in esophageal cancer patients // Radiat Oncol. 2021. Vol. 16, N 1. ID 220. doi: 10.1186/s13014-021-01950-y
27. Liang B., Yan H., Tian Y., et al. Dosiomics: Extracting 3D spatial features from dose distribution to predict incidence of radiation pneumonitis // Front Oncol. 2019. Vol. 9. ID 269. doi: 10.3389/fonc.2019.00269
28. Liang B., Tian Y., Chen X., et al. Prediction of radiation pneumonitis with dose distribution: A convolutional neural network (CNN) based model // Front Oncol. 2020. Vol. 9. ID 1500. doi: 10.3389/fonc.2019.01500
29. Adachi T., Nakamura M., Shintani T., et al. Multi-institutional dose-segmented dosiomic analysis for predicting radiation pneumonitis after lung stereotactic body radiation therapy // Med Phys. 2021. Vol. 48, N 4. P. 1781–1791. doi: 10.1002/mp.14769
30. Zheng X., Guo W., Wang Y., et al. Multi-omics to predict acute radiation esophagitis in patients with lung cancer treated with intensity-modulated radiation therapy // Eur J Med Res. 2023. Vol. 28, N 1. ID 126. doi: 10.1186/s40001-023-01041-6

AUTHORS' INFO

*** Mikhail E. Ivannikov,** MD;
address: 86 Profsoyuznaya str., 117997, Moscow, Russia;
ORCID: 0009-0007-0407-0953;
eLibrary SPIN: 3419-2977;
e-mail: ivannikovmichail@gmail.com
Nikolay V. Nudnov, MD, Dr. Sci. (Medicine), Professor;
ORCID: 0000-0001-5994-0468;
eLibrary SPIN: 3018-2527;
e-mail: nudnov@rncrr.ru
Vladimir M. Sotnikov, MD, Dr. Sci. (Medicine), Professor;
ORCID: 0000-0003-0498-314X;
eLibrary SPIN: 3845-0154;
e-mail: vmsotnikov@mail.ru
Elina S-A. Shakhvalieva, MD;
ORCID: 0009-0000-7535-8523;
e-mail: shelina9558@gmail.com

ОБ АВТОРАХ

*** Иванников Михаил Евгеньевич;**
адрес: Россия, 117997, Москва, ул. Профсоюзная, д. 86;
ORCID: 0009-0007-0407-0953;
eLibrary SPIN: 3419-2977;
e-mail: ivannikovmichail@gmail.com
Нуднов Николай Васильевич, д-р мед. наук, профессор;
ORCID: 0000-0001-5994-0468;
eLibrary SPIN: 3018-2527;
e-mail: nudnov@rncrr.ru
Сотников Владимир Михайлович, д-р мед. наук, профессор;
ORCID: 0000-0003-0498-314X;
eLibrary SPIN: 3845-0154;
e-mail: vmsotnikov@mail.ru
Шахвалиева Элина Саид-Аминовна;
ORCID: 0009-0000-7535-8523;
e-mail: shelina9558@gmail.com

Aleksandr A. Borisov, MD;
ORCID: 0000-0003-4036-5883;
eLibrary SPIN: 4294-4736;
e-mail: aleksandrborisov10650@gmail.com
Vasiliy V. Ledenev, MD, Cand. Sci. (Medicine);
ORCID: 0000-0002-2856-2107;
eLibrary SPIN: 2791-0329;
e-mail: Ledenevvv007@gmail.com
Aleksei Yu. Smyslov, Cand. Sci. (Engineering);
ORCID: 0000-0002-6409-6756;
eLibrary SPIN: 9341-0037;
e-mail: smyslov.ay@gmail.com
Alina V. Ananina;
ORCID: 0009-0002-4562-9729;
eLibrary SPIN: 9699-7690;
e-mail: vastruhina.a.v@yandex.ru

Борисов Александр Александрович;
ORCID: 0000-0003-4036-5883;
eLibrary SPIN: 4294-4736;
e-mail: aleksandrborisov10650@gmail.com
Леденёв Василий Владимирович, канд. мед. наук;
ORCID: 0000-0002-2856-2107;
eLibrary SPIN: 2791-0329;
e-mail: Ledenevvv007@gmail.com
Смыслов Алексей Юрьевич, канд. техн. наук;
ORCID: 0000-0002-6409-6756;
eLibrary SPIN: 9341-0037;
e-mail: smyslov.ay@gmail.com
Ананьина Алина Валентиновна;
ORCID: 0009-0002-4562-9729;
eLibrary SPIN: 9699-7690;
e-mail: vastruhina.a.v@yandex.ru

* Corresponding author / Автор, ответственный за переписку